Electrochemical reduction of nalidixic acid at glassy carbon electrodemodified with multi-walled carbon nanotubes

Reference:

Patiño Yolanda, Pilehvar Sanaz, Díaz Eva, Ordóñez Salvador, De Wael Karolien.- Electrochemical reduction of nalidixic acid at glassy carbon electrodemodified with multi-walled carbon nanotubes

Journal of hazardous materials - ISSN 0304-3894 - (2016), p. 1-11

Full text (Publishers DOI): http://dx.doi.org/doi:10.1016/j.jhazmat.2016.10.023

Title: ELECTROCHEMICAL REDUCTION OF NALIDIXIC ACID AT GLASSY CARBON ELECTRODE MODIFIED WITH MULTI-WALLED CARBON NANOTUBES

Author: Yolanda Patiño Sanaz Pilehvar Eva Díaz Salvador Ordóñez Karolien De Wael

PII: S0304-3894(16)30920-7
DOI: http://dx.doi.org/doi:10.1016/j.jhazmat.2016.10.023
Reference: HAZMAT 18104

To appear in: *Journal of Hazardous Materials*

Received date: 14-7-2016
Revised date: 25-9-2016
Accepted date: 12-10-2016

Please cite this article as: Yolanda Patiño, Sanaz Pilehvar, Eva Díaz, Salvador Ordóñez, Karolien De Wael, ELECTROCHEMICAL REDUCTION OF NALIDIXIC ACID AT GLASSY CARBON ELECTRODE MODIFIED WITH MULTI-WALLED CARBON NANOTUBES, Journal of Hazardous Materials http://dx.doi.org/10.1016/j.jhazmat.2016.10.023

ELECTROCHEMICAL REDUCTION OF NALIDIXIC ACID AT GLASSY CARBON ELECTRODE MODIFIED WITH MULTI-WALLED CARBON NANOTUBES

Yolanda Patiño[a], Sanaz Pilehvar[b], Eva Díaz[a], Salvador Ordóñez[a*], Karolien De Wael[b]

[a]*Department of Chemical and Environmental Engineering, University of Oviedo, Faculty of Chemistry, Julián Clavería s/n, 33006 Oviedo, Spain*
[b] *AXES research group, Department of Chemistry, University of Antwerp, Groenenborgerlaan 171, 2020 Antwerp, Belgium*

E-mail: sordonez@uniovi.es

Graphical abstract

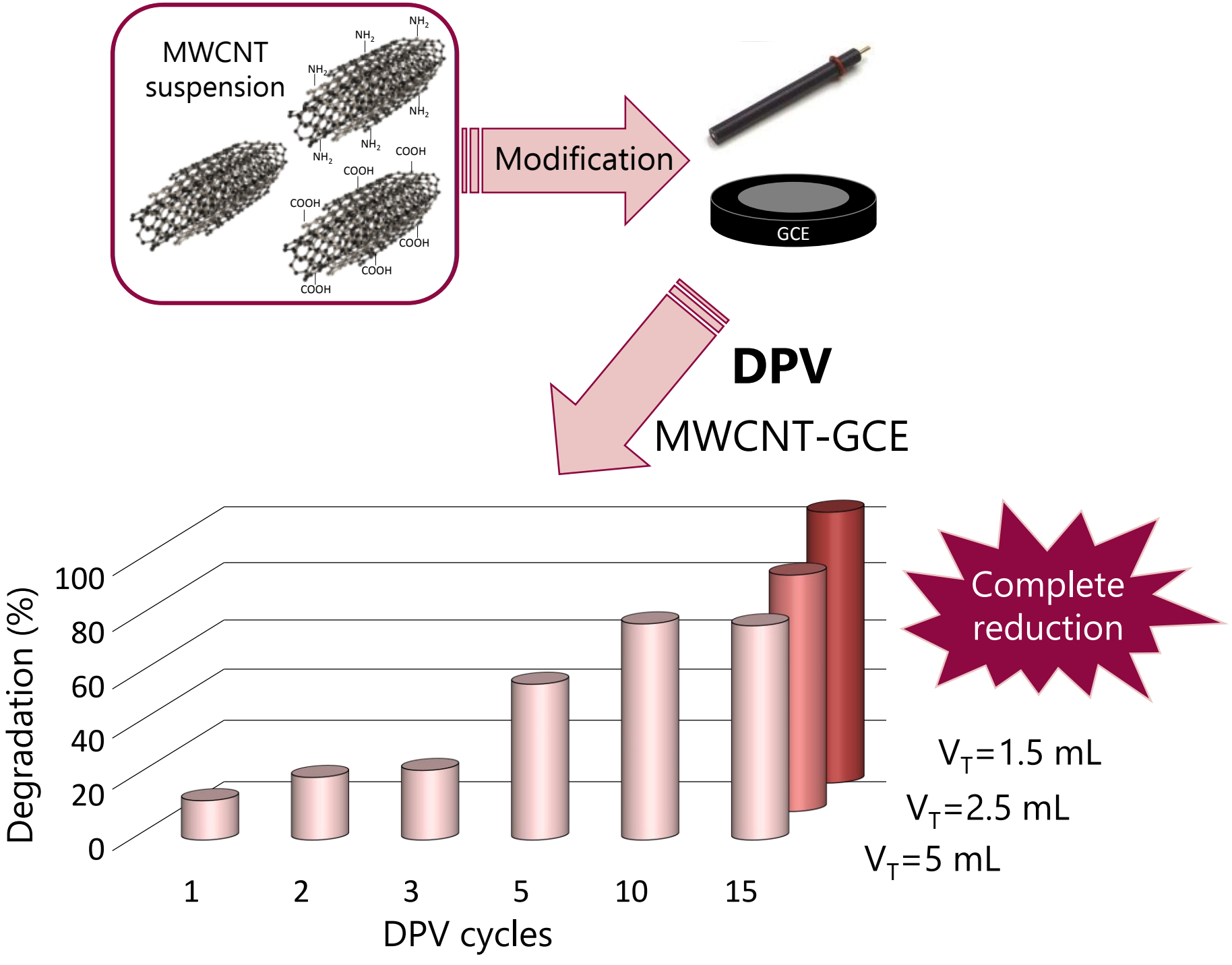
MWCNT
suspension
NH2
COOH
Modification
GCE
DPV
MWCNT-GCE
Degradation (%)
0
20
40
60
80
100
1
2
3
5
10
15
DPV cycles
Complete
reduction
VT=1.5 mL
VT=2.5 mL
VT=5 mL

HIGHLIGHTS

- MWCNTs present electrocatalytic effect toward nalidixic acid reduction
- The nalidixic acid reduction is an irreversible process
- The process is controlled by adsorption and not by difussion
- A total degradation is obtain using MWCNT modified glassy carbon electrode
- Two different sub-products were identified based on the elemental composition

Abstract

The aqueous phase electrochemical degradation of nalidixic acid (NAL) is studied in this work, using cyclic voltammetry (CV) and differential pulse voltammetry (DPV) as instrumental techniques. The promotional effect of multi-walled carbon nanotubes (MWCNT) on the the performance of glassy carbon electrodes is demonstrated, being observed that these materials catalyze the NAL reduction. The effect of surface functional groups on MWCNT -MWCNT-COOH and MWCNT-NH_2 – was also studied. The modification of glassy carbon electrode (GCE) with MWCNT leads to an improved performance for NAL reduction following the order of MWCNT > MWCNT-NH_2 > MWCNT-COOH. The best behavior at MWCNT-GCE is mainly due to both the increased electrode active area and the enhanced MWCNT adsorption properties.

The NAL degradation was carried out under optimal conditions (pH = 5.0, deposition time = 20 s and volume of MWCNT =10 μL) using MWCNT-GCE obtaining an irreversible reduction of NAL to less toxic products. Paramaters as the number of DPV cycles and the volume/area (V/A) ratio were optimized for maximize pollutant degradation. It was observed that after 15 DPV scans and V/A=8, a complete reduction was obtained, obtaining two sub-products identified by liquid chromatography-mass spectrometry (LC-MS).

Keywords: quinolones; degradation; cyclic voltammetry; differential pulse voltammetry; micropollutants

1. Introduction

In recent years, the production and consumption of pharmaceutical products have exponentially increased, leading to an increase of the release to different kinds of water streams [1]. Many of these drugs are antibiotics, which are non-biodegradable, toxic and refractory to degradation by conventional chemical or biological methods [2].

Nalidixic acid (NAL) is a non-biodegradable antibacterial agent firstly synthesized by Lesher et al. in 1960 and used in the treatment of gram-negative urine tract infections. Because of this use, this chemical is released to the environment and frequently identified in surface water and wastewater [3-6]. Due to its release to water effluents and its inefficient removal in sewage treatment plants, the concerns about its effects on human health have increased. When it is present at low concentrations, the compound acts as bacteriostatic, inhibiting bacterial growth and reproduction, while at high concentrations it exhibits bactericidal effects [7]. Besides, when the antiobiotic is consumed unnecessarily and prolonged in time may affect the immune system and act as toxic compound [8].

Although there are many studies about the determination of nalidixic acid by several techniques, such as spectroscopy [9], fluorescence [10, 11], phosphorescence [12] and chromatography [13-15], reports on its degradation are rather scarce.

Nalidixic acid has been found in surface water at very low concentration in the order of 10 $ng \cdot L^{-1}$ to 2 $\mu g \cdot L^{-1}$ [16]. Due to its low concentration in water, and in order to facilitate the removal step, a two-step process by pre-concentration and removal is proposed in a previous work [17]. The NAL pre-concentration was studied by adsorption onto carbon materials – activated carbon, high surface area graphite and multiwall carbon nanotubes – obtaining the best results using carbon nanotubes [17]. Once the pollutant is concentrated and the volume of water to be treated has been reduced, the stage of degradation of NAL could be implemented.

Different advance oxidation processes (AOPs) have been tested by other authors. Sirtori et al., [5] studied the removal of NAL by solar photo-fenton reaction, Pollice et al., [7] reported its degradation by an integrated MBR-ozonation system and the photodegradation of NAL has been considered by Petronella et al., [18] and Vargas et al., [19].

Although AOPs are promising removal procedures, these techniques require a large capital, and in many cases, a complex chemistry must be tailored to specific application. Besides, the choice of reagent is a critical parameter due to the possible formation of by-products.

Therefore, electrochemical treatment is an interesting alternative. Electrochemical techniques have been commonly used as analytical methods for the determination of different pollutants in water. In this work the novelty of using this technique as a method of degradation of pollutants is proposed, since this technology offers relevant advantages: instrumental simplicity, moderate costs, use of clean reactants – electrons- and possibility to operate at ambient temperature and pressure [20, 21].

Conventional electrodes used in electrochemical methods present low surface areas and weak interaction with the organic compound. This fact leads to low sensitivity when conventional electrodes are used for analytical purposes, or low efficiencies when used for pollutant abatement. It is an ongoing challenge to develop proper materials for electrode surface modification increasing the performance of these devices [22, 23]. As an alternative for electrode modification, carbonaceous materials, and in particular carbon nanotubes (CNTs) offer great potential due to their high electrical conductivity, high mechanical resistance, good chemical stability and high surface area [24-25]. An increased electrode surface area improves the electrochemical response and provides the electrode with anti-fouling properties [25]. Besides, the electron transfer reactions improve by using short carbon nanotubes comparing with long MWCNT and it may be affected by the functional groups present at carbon nanotubes [26-29]. The electrocatalytic effect has been attributed to the activity of edge-plane-like graphite sites at the carbon nanotubes ends [27, 30]

The main objective of this work is the study of the degradation of nalidixic acid by electrochemical techniques using electrodes modified with carbon nanotubes. To the best of our knowledge, electrochemical degradation of NAL has not been reported yet. The variables which influence the process (pH, deposition time and volume of MWCNT) were optimized. Three kinds of MWCNT were used: non- functionalized (MWCNT), functionalized with carboxylic (MWCNT-COOH) and amine (MWCNT-NH_2) groups in order to investigate the effect of functional groups on the degradation process. Experiments were performed using cyclic voltammetry and differential pulse voltammetry. These techniques allow a systematic study of the electrochemical degradation of this kind of pollutants, determining the effect of both electrode properties and operation conditions in this electrochemical reaction.

2. Materials and Methods

2.1. Chemicals and reagents

Nalidixic acid was purchased from Duchefa, Biochemie B.V. (purity > 99.4).

Three multi-walled carbon nanotubes have been used, all manufactured by DropSense: non-functionalized multi-walled carbon nanotubes (MWCNT; S_{BET}=277 m^2/g and V_{meso}=2.50 cm^3/g), functionalized with –COOH groups (MWCNT-COOH; S_{BET}=273 m^2/g and V_{meso}=1.32 cm^3/g), and functionalized with –NH_2 groups (MWCNT-NH_2; S_{BET}=293 m^2/g and V_{meso}=1.38; cm^3/g). Their morphological properties have been reported in a previous work (Table S1) [31].

Phosphate buffer (PBS) solutions of different pH were prepared by mixing the corresponding amounts of sodium chloride (NaCl), potassium chloride (KCl), potassium phosphate monobasic (KH_2PO_4) and sodium phosphate dibasic (Na_2HPO_4).

Potassium hexacyanoferrate (II) ($K_4[Fe(CN)_6]$) was purchased from Merck and potassium hexacyanoferrate (III) ($K_3[Fe(CN)_6]$) was obtained from Sigma-Aldrich, Belgium.

2.2. Instrumentation

All electrochemical experiments, cyclic voltammetry and differential pulse voltammetry, were performed using a μ-Autolab Potentiostat/Galvanostat PGSTAT20, type II controlled by NOVA 1.10 software package (ECO Chemie, Utrecht, The Netherlands). The three electrode system consists of a glassy carbon (GCE) as working electrode, saturated calomel (SCE) as the reference electrode and platinum (Pt) as an auxiliary electrode. Prior to the electrochemical measurements, the solution were purged for 20 min with purified nitrogen gas and a constant potential was applied to enable the deposition of NAL on the working electrode surface.

A Cary 100 UV-Vis spectrophotometer (Varian Inc. USA) was employed for the detection of NAL at a wavelength of 258 nm. Calibration was established using five standards with the r^2 coefficient of determination higher than 0.995. The by-products degradation were determined by high performance liquid chromatography with mass spectrometry detector (LC-MS), using a UPLC Agilent 6460.

2.3. Preparation of the modified electrodes

Before modification, the GCE was polished with 0.1 and 0.05 μm aluminum slurry, rinsed with distilled water and then ultrasonicated in water and dried in the air.

MWCNTs solution was prepared by dispersing MWCNTs into dimethylformamide (DMF) with concentrations of 0.25 $g \cdot L^{-1}$ by ultrasonication to obtain a well-dispersed suspension, according to the process developed by García-González et al.[31]. Next, an amount of 5, 10 or 15 μL of the suspension was deposited on the GCE area and then, dried under room temperature before the electrochemical measurements.

2.4. Electrode characterization

Scanning electron microscopy (SEM) was performed with a QUANTA 250 FEG SEM (FEI, Hillsboro, Oregon, USA) and in a JEOL-6610LV SEM (Tokyo, Japan). SEM was used to characterize the working electrodes modified with the MWCNTs solutions.

The surface area of the MWCNTs modified GCE and the bare GCE were obtained by cyclic voltammetry (CV) using a 1 mML^{-1} $K_3[Fe(CN)_6]$ solution at different scan rates.

2.5. Reaction procedure

The degradation process was carried out in the cell using the three electrode system with MWCNT-GCE as working electrode by applying a potential from -1.15 to -0.45 V by DPV. The process was studied at diffeten V/area (solution volume/electrode area) ratios and the swift potential was applied several times until the maximum degradation was reached. Prior to the swift potential a constant potential was applied with the aim of promoting the NAL adorption on the electrode surface, thereby achieving a greater degradation.

3. Results and Discussion

3.1. Characterization of the modified electrodes

The MWCNTs modified GCEs were first characterized using SEM. Fig. 1 and S1 show the SEM images obtained for the different working electrodes at two different magnifications. As shown in Fig. 1 (B), the modified electrode presents an interwoven mesh of nanotubes, with different thin layers forming a porous structure. Functionalized MWCNT modified electrodes (Fig. 1 (C) and (D)), resulted in a more heterogeneous surface. In the case of MWCNT-COOH modified GCE (Fig.1(C), carbon nanotubes formed bubble like structures, where the carbon nanotubes are clustered. For MWCNT-NH_2 (Fig. 1(D)), the MWCNT density presents differences

between the perimeter zone, where the numbers of layers and therefore the density of MWCNT-NH_2 is less, and the central zone, where the density is higher (Figure S2). The film thickness and density of multi-wall carbon nanotubes were also calculated (Fig. 2 and Table 1). MWCNT modified GCE presents the most uniform film thickness, with different MWNCT layers with a practically constant density, where the electrocatalytic reduction of NAL can take place (Fig. 2 (A)). In the case of MWCNT-COOH a film with constant thickness was obtained over the entire surface, but the presence of buble structures makes the surface as no-uniform (Fig. 2 (B)). Finally in the case of MWCNT-NH_2, the film thickness is not constant along the whole radius, and it is 2.5 times higher in the central zone than in the perimeter zone, which involves a difference in the density of carbon nanotubes (Table 1). The distributions obtained for the working electrodes correspond to those achieved in other works, where MWCNT leads to a uniform surface, which makes it as the best option to modify the electrode surface [28, 33, 34].

The active surface area of the different electrodes is estimated according to the Randles-Sevcik equation (Eq. 1) (at 20 °C) for a reversible process (Table 1)[35].

$$i_p = 2.69 \times 10^5 \, n^{3/2} \, A \, C_0 \, {D_R}^{1/2} \, \nu^{1/2} \qquad (1)$$

where i_p is the anodic peak current, n is the number of electron transfer (n=1), A is the surface area of the electrode, C_0 is the concentration of potassium ferrocyanide (1 mM), D_R is the diffusion coefficient (D_R= 7.6 x 10^{-6} cm^2s^{-1}) and ν is the scan rate. From the slope of the i_p *vs* $\nu^{1/2}$, the value of A can be obtained.

The electrode surface area obtained follows the order MWCNT >> MWCNT-COOH > MWCNT-NH_2 > Bare. As it is clear from these values, MWCNT-GCE presents the highest surface area, three times greater than the bare GCE; whereas modified GCE with functionalized MWCNT results in a similar surface area slightly higher compared to bare-GCE, in agreement with other authors [33, 36-38]. The increased effective surface area after modification of GCE

with MWCNTs could lead to an enhancement in the NAL pre-concentration, and, consequently, to a higher NAL electrochemical degradation.

3.2. Electrochemical response by CV and DPV

The cyclic voltammetric responses of 1×10^{-5} M NAL in phosphate-buffered saline (PBS; pH=7) at bare GCE are shown in Fig. 3. The concentration was selected both considering the detection limits of the technique, as well as typical concetration both in wastewaters and in the streams coming from the cleaning of adsorption beds used in water purification [17]. No reduction/oxidation peak was observed at GCE in a blank solution. In the presence of 1×10^{-5} M NAL, a small reduction wave appeared at -0.91 V (vs. SCE). The absence of the oxidative peak on the reverse scan suggests the irreversible nature of the electrode process, which is corroborated by previous works [39].

To evaluate the electrocatalytic effect of MWCNT on the NAL reduction, DPV scans were performed at bare-GCE and MWCNT-GCE. As despicted in Fig. 4, the peak current related to NAL (1×10^{-5} M) increases when the surface of GCE is modified with MWCNTs. Same results were obtained by other studies about the electrochemical response of different antibiotics. For example, Rezaei et al.,[33] did not obtain an oxidation peak for noscapine at the bare electrode, on the contrary, two oxidation peaks were obtained using a MWCNT modified electrode by cyclic voltammetry. Moyo et al., [38] obtained also better results with MWCNT for the electro-oxidation of triclosan, with a peak area approximately twice bigger compared to that obtained at bare GCE by cyclic voltammetry and differential pulse voltammetry. The increased surface area of the electrode after the modification with carbon nanotubes results in higher catalytic activity and adsorption capability of the surface and a higher response making carbon nanotubes as a good alternative for NAL degradation.

The relation between the peak current and the concentration of NAL was obtained by DPV using MWCNT-GCE. The peak current increases with increase in the NAL concentration, and

two different ranges were obtained (Fig. 5). The first linear range is between 0.0001-0.05 µM and the second linear range is from 0.1 µM to 50 µM, both with a regression coefficient, higher than 0.996. A similar trend has been observed by other authors by different electrochemical techniques for paracetamol [40], ascorbic acid and caffeine [41]. This phenomena can be explained through the formation of a sub-monolayer in the first linear part, where NAL molecules are adsorbed inside pores and between the different layers , followed by the formation of a NAL monolayer in the second part of the calibration plot, after adsorption on the electrode surface [40].

3.3. Optimization of experimental variables

3.3.1. pH

The effect of pH on the DPV response was studied in PBS in the range of 3.0 - 9.0, to obtain the optimum pH value for NAL reduction using MWCNT-GCE as working electrode (Fig. 6). At the same time, it is important to take into account the NAL forms at different pH. Lorphensri et al., [42] found that at pH<4.5 and pH>8.0, NAL is present in its neutral and anionic form respectively. At 4.5<pH<8.0, NAL is present in both neutral and anionic form at differents proportions depending on the pH. The neutral form should be more electrochemically active than the anionic form, so a pH close or less than 4.5 would be the best option. Taking into account the peak current obtained at different pH, it reaches a maximum value at pH 5.0, after that, the peak current decreases, observing a significant influence of the pH on the reduction of NAL. Conferring to Lorphensri et al., [42] at this pH (pH 5.0) the 95% of NAL is present in the neutral form.

Therefore, according to the different results, pH 5.0 was chosen as the optimum and it was used for the following experiments.

3.3.2. Deposition time

Initially, a constant potential is applied in order to favor the NAL adsorption on the electrode surface. For this reason, the effect of deposition time was studied ranging from 10 to 1200 s. Fig. 7 shows that the peak current decreases for a deposition time higher than 20 s. No further change in peak current was observed with the increasing time higher than 20 s. In most cases, peak intensity remains constant after a certain accumulation time, contrary than the result obtained in this work [43-45]. A decrease in the peak intensity with time was also observed by a few number of authors and it is attributed to the formation of multilayer on the electrode surface, which reaches a maximum thickness due to the lack of stability of the MWCNT [46, 47]. In this way, part of the nanotubes can detach the electrode, decreasing the concentration of carbon nanotubes in the electrode surface, and as consequence, the amount of NAL adsorbed.

3.3.3. Volume of MWCNT suspension

The effect of varying the volume of MWCNT suspension was studied in the range from 5 to 15 µL. It was observed that increasing the MWCNTs volume, the reduction peak current increases until 10 µL and then, the current decreases drastically. This effect can be explained in relation to the film thickness, which was obtained from the cross section SEM images (Figure S3). When the film is too thin ($\leq$ 0.9 µm), the amount of NAL adsorbed is less and therefore, the reduction current is suppressed. When the film is too thick ($\geq$2.87 µm), the film conductivity is reduced and the MWCNT film becomes unstable, resulting in a lower value of the peak current. Therefore, 10 µL of MWCNTs, with a thickness close to 2 µm, is chosen as the optimal dosage in the present study. The same trend was obtained in different studies for the detection of pharmaceutical products using GCE modified with MWCNTs [37, 48, 49].

After optimization of all the variables that can influence the process, the selected optimum conditions were: pH equal to five, 20 s of deposition time and 10 µL of MWCNT to drop on the GCE surface. The rest of the experiments were done at optimal conditions.

3.4. Scan rate studies

The relationship between peak current and scan rate gives information about if the electrochemical process is controlled by adsorption or by difussión. Scan rate studies were carried out under optimal conditions, and it was found that the anodic peak current of NAL is linear to scan rate, which indicates that the electrode process is controlled by adsorption [43, 50] (Eq. 2).

$$ip\ (\mu A) = 6.9916\ \nu\ (V \cdot s^{-1}) + 0.0229, \quad r^2 = 0.994 \qquad (2)$$

It was also confirmed by the relationship between log Ip and log v; which follows the next equation:

$$\log ip\ \ (\mu A) = 0.8916 \log \nu\ \ (V \cdot s^{-1}) + 0.7299, \quad r^2 = 0.9974 \qquad (3)$$

The slope is closed to the theoretically expected value 1.0 which confirms adsorption controlled nature of the electrode process [50]

From the scan rate it is also possible to obtain information about the reversible/irreversible nature of the process. As the scan rate increases, the peak potential is shifted to more negative value with increase in current, which confirms the irreversible nature of the reduction process [37, 51].

3.5. Effect of functional groups of MWCNT

In order to study the effect of the nature of the functional groups present at the MWCNTs on the electrochemical reduction of NAL, both MWCNT-COOH and MWCNT-NH_2 modified glassy carbon electrodes were tested by DPV. The peak intensities of 1×10^{-5} M NAL obtained at different modified electrodes are compared in Fig. 8. All electrodes modified with MWCNTs

showed the redox process of NAL. MWCNT presents the highest value for the peak current, which can be explained by the high adsorption capacity of NAL onto MWCNTs. The deposition step is very important since the amount of reduced NAL increases as the amount of adsorbed NAL on the electrode surface increases. The adsorption of NAL onto these carbon nanotubes has been studied in previous works by batch and fixed bed adsorption [17, 31]. The adsorption capacity is dependent on both, morphological and chemical properties of the different MWCNT (Table S1). Regarding to the morphological properties, MWCNT is the material with the highest mesoporous volume and pore width (Table S1). For this reason a greater amount of NAL is adsorbed on the electrode surface during the deposition time when MWCNT is ussed to modified the GCE, and as consequence the peak current is higher for this working electrode. On the other hand, the interaction should be worse on the surface of MWCNT-COOH, the material with the lower PZC (Table S1). Although MWCNT-NH_2 presents the highest PZC, it is similar than the obtained for MWCNT, so that this difference is not enough to exceed the adsorption obtained with MWCNT, which presents the best morphological properties (Table S1). The adsorption capacity obtained by batch adsorption experiments for the different MWCNT followed the order: MWCNT>MWCNT-NH2>MWCNT-COOH, fitting clearly with the results obtained in this work, which justifies that the adsorption stage during the constant potential plays an important role in efficiently reducing NAL.

The negative effect of functionalized-MWCNT on the NAL degradation can be explained since the functional groups onto MWCNTs might block the adsorption of NAL molecules [52]. Once the importance of the adsorption process on the NAL degradation has been demonstrate, it is important to note that the π- π interaction plays an important role, where the carbon materials act as electron donor and the aromatic rings of NAL as electron acceptor. This allows partially to explain the poor performance of MWCNT-COOH compare with MWCNT-NH_2. The oxygen groups present in MWCNT-COOH make the π-π interaction more difficult due to the modification of the electron density at the carbon nanotubes surface [53]. In addition, the

nitrogen content in MWCNT-NH_2 act as electron donor, increasing its affinity for NAL [54]. Besides, due to the hydrophilic character of MWCNT-COOH (more than MWCNT-NH_2), these groups could favor the formation of hydrogen bonds with water molecules, which causes a decrease in the amount of NAL adsorbed on the electrode surface leading to less degradation [31].

The current intensity/area (i/A) ratio of different electrodes were compared in order to determine if both parameters are related. The i/A ratio follows the order: MWCNT>MWNCT-COOH>MWCNT-NH_2>Bare, which confirms that the chemical nature of the nanotubes positively affects the NAL reduction [55].

The peak potential of NAL reduction are all shifted, in the order: MWCNT (-0.84 V) < MWCNT-NH_2 (-0.82 V) < MWCNT-COOH (-0.80 V) < Bare (-0.79 V) (Fig. 8), which proves the existence of electro-catalytic activity of these modified GCE [56]. Bi et al., [55] obtained similar result in the study of the effect of functional groups of MWCNT for the detection of ascorbic acid, dopamine and uric acid. The study employed MWCNT, MWCNT-COOH and MWCNT-OH, where the highest electrocatalytic activity was obtained by MWCNT.

3.6. Degradation of NAL by DPV and degradation products

The electrochemical degradation of NAL was performed by DPV using MWCNT-GCE as working electrode, under the optimum operating conditions in a potential range of -0.3 to -1.15 V. The experiments were performed for 2, 3, 4, 5, 10 and 15 DPV scans (add the time equivalent of 15 DPV) and the final concentration was analyzed by UV-Vis spectrophotometer in order to estimate the NAL degradation in %. A V/A ratio equal to 28 and an initial NAL concentration of 1×10^{-5} M of NAL were selected. The initial concentration was selected taking into account the detection limits of this technique and the concentration factor obtained in a previous work, where the pre-concentration of NAL was studied, since the degradation is a part of a two-step

process (pre-concentration + degradation) [17]. After one DPV, the degradation of NAL in the solution was calculated to be 12.5 %. In order to increase the NAL removal, repetitive DPV were carried out. With increasing the number of DPVs, more NAL deposition on the electrode surface takes place, which could increase the amount of reduced NAL.

Fig. 9 (A) shows the effect of several DPV scans on the NAL degradation (%). The degradation increases linearly (r^2> 0.9) from 12.5 % to 80 % as the number of DPV increase, up to 10 DPV. After 10 DPV , the final concentration remains constant with no further increase of the NAL degradation, which may be due to a saturation of the electrode surface. If the electrode surface is saturated, the NAL adsorption onto the surface is not possible and as consequence, the MWCNT cannot act as electro-catalyst for its further reduction.

In order to increase the NAL degradation, the V/A ratio was decreased until obtaining the maximum NAL reduction. By reducing the total volume (same initial concentration and electrode area), the mass of NAL in the solution decreases, therefore the saturation of the electrode will take place after more DPV . The same effect will take place if the electrode area increases. Three different V/A ratio containing 28, 14 and 8 were tested at 15 DPV to ensure that the maximum NAL degradation is obtained. As can be seen in Fig. 9 (B) the maximum NAL degradation was obtained for a V/A ratio equal to eight, where all the NAL has been reduced to the sub-products.

The sub-products have been identified by LC-MS through the final solution under the conditions where a complete degradation was obtained. The disappearance of the peak corresponding to the nalidixic acid confirms its complete degradation. On the other hand, the appearance of two new peaks indicate the formation of subproducts where the highest intensity was obtained for m/z ratios equal to 223 and 269. At this point, it is important to emphasize that there are not any study reported about the sub-products resulted from the electrochemical reduction of NAL. Their identification was based on the elemental composition for the measured accurate m/z of the protonated molecules. The proposed structures and

pathways are shown in Figs. 10 and 11. The methyl-pyridine ring remained unchanged in all of them. In the first step, the double bond cleavage of the second ring takes place by water addition in both cases. In the second step, a new water molecule causes the cleavage ring with the addition of an oxygen in C_2 or C_3 depending on the mechanism propoused. The products P_1 and P_3 are obtained by reduction of the less stable carbonyl group. The loss of the carboxylic group generates the products P_2 and P_4 corresponding with the m/z=222. In the pathway 1, the previous molecule has two carboxylic groups so that, this loss takes place in the less stable bond, corresponding with the C-N bond.

Regarding to the by-products toxicity, the same products or in some cases very similar products were obtained in other works by different degradation techniques [5, 18, 57]. These authors determined that the toxicity of the final solution is mainly due to the residual concentration of NAL, rather than by-products.

4. Conclusions

The electrochemical degradation of nalidixic acid was studied by differential pulse voltammetry. After the optimization of the experimental variables and previous to the degradation process, modified electrodes with three different multi wall carbon nanotubes – MWCNT, MWCNT-COOH and MWCNT-NH_2 – were tested.

The electrocatalytic effect towards NAL reduction with modified electrodes was compared to the situation at a non modified glassy carbon electrode, following the order: MWCNT > MWCNT-NH_2 > MWCNT-COOH. MWCNT is nanostructured allowing an efficient adsorption and preconcentration of NAL on the electrode surface during the deposition step, yielding higher current responses by CV and DPV.

A complete reduction of NAL has been obtained with a MWCNT modified GCE, under the optimal conditions of 15 DPV scans and the V/A ratio equal to 8. The complete degradation has been confirmed by UV-VIS spectrophotometer and two different sub-products have been identified by LC-MS.

This study shows the direct application of MWCNT modified GCE for the complete degradation of nalidixic acid and offers a green alternative, a simple fabrication procedure and an easy regeneration of electrode surface, which only needs to be polished for a new use.

Acknowledgements

This work was supported by the Spanish Government (contract CTQ2011-29272-C04-02) and by the Government of the Principality of Asturias (contract FC-15-GRUPIN14-078). Y. Patiño thanks the Government of the Principality of Asturias for a Ph.D. fellowship (Severo Ochoa Program). S. P. and K. D. W. are thankful to UA for DOCPRO financial support.

References

[1] V. Homem, L. Santos, Degradation and removal methods of antibiotics from aqueous matrices – A review, J. Environ. Manage., 92 (2011) 2304-2347.

[2] L. Feng, E.D. van Hullebusch, M.A. Rodrigo, G. Esposito, M.A. Oturan, Removal of residual anti-inflammatory and analgesic pharmaceuticals from aqueous systems by electrochemical advanced oxidation processes. A review, Chem. Eng. J., 228 (2013) 944-964.

[3] S.A. R. Gleckman, D.W. Joubert, S.J. Matthews, Drug therapy reviews: nalidixic acid,

Am. J. Hosp. Pharm., 36 (1979) 1071-1076.

[4] G.Y. Lesher, E.J. Froelich, M.D. Gruett, J.M. Bailey, R.P. Brundage, 1,8-naphthyridine derivatives: a new class os chemotherapeutic agents, J. Med. Pharm. Chem., 5 (1962) 1063.

[5] C. Sirtori, A. Zapata, W. Gernjak, S. Malato, A. Lopez, A. Agüera, Solar photo-Fenton degradation of nalidixic acid in waters and wastewaters of different composition. Analytical assessment by LC–TOF-MS, Water Res., 45 (2011) 1736-1744.

[6] L. Ge, J. Chen, X. Wei, S. Zhang, X. Qiao, X. Cai, Q. Xie, Aquatic Photochemistry of Fluoroquinolone Antibiotics: Kinetics, Pathways, and Multivariate Effects of Main Water Constituents, Environ. Sci. Technol., 44 (2010) 2400-2405.

[7] A. Pollice, G. Laera, D. Cassano, S. Diomede, A. Pinto, A. Lopez, G. Mascolo, Removal of nalidixic acid and its degradation products by an integrated MBR-ozonation system, J. Hazard. Mater., 203–204 (2012) 46-52.

[8] M.S. Ibrahim, I.S. Shehatta, M.R. Sultan, Cathodic adsorptive stripping voltammetric determination of nalidixic acid in pharmaceuticals, human urine and serum, Talanta, 56 (2002) 471-479.

[9] E.F. Salim, I.S. Shupe, Qualitative and quantitative tests for nalidixic acid, J. Pharm. Sci., 55 (1966) 1289-1290.

[10] J.A.M. Pulgarin, A.A. Molina, P.F. López, Direct determination of nalidixic acid in urine by matrix isopotential synchronous fluorescence spectrometry, Talanta, 43 (1996) 431-438.

[11] M.L. Wang, S.C. Chen, J.C. Lien, S.C. Kuo, Determination of nalidixic acid by fluorometry with sodium borohydride and hydrogen peroxide, J. AOAC Int., 85 (2002) 572-575.

[12] L.F. Capitán-Vallvey, F. Ojeda, M. Del Olmo, R. Avidad, A. Navalón, T. Vo-Dinh, Use of transmitted room-temperature phosphorescence to improve nalidixic acid determination, Appl. Spectrosc., 52 (1998) 101-105.

[13] V.R. Bari, U.J. Dhorda, M. Sundaresan, Simultaneous estimation of nalidixic acid and metronidazole in dosage forms using packed column supercritical fluid chromatography, Anal. Chim. Acta, 376 (1998) 221-225.

[14] T. Pérez-Ruiz, C. Martínez-Lozano, A. Sanz, E. Bravo, Separation and simultaneous determination of nalidixic acid, hydroxynalidixic acid and carboxynalidixic acid in serum and urine by micellar electrokinetic capillary chromatography, J. Chromatogr. B, 724 (1999) 319-324.

[15] M. Horie, K. Saito, Y. Hoshino, N. Nose, E. Mochizuki, H. Nakazawa, Simultaneous determination of nalidixic acid, oxolinic acid and piromidic acid in fish by high-performance liquid chromatography with fluorescence and uv detection, J. Chromatogr. A, 402 (1987) 301-308.

[16] D.W. Kolpin, E.T. Furlong, M.T. Meyer, E.M. Thurman, S.D. Zaugg, L.B. Barber, H.T. Buxton, Pharmaceuticals, hormones, and other organic wastewater contaminants in U.S. streams, 1999-2000: a national reconnaissance, Environ. Sci. Technol., 36 (2002) 1202-11.

[17] Y. Patiño, E. Díaz, S. Ordóñez, Pre-concentration of nalidixic acid through adsorption–desorption cycles: Adsorbent selection and modeling, Chem. Eng. J., 283 (2016) 486-494.

[18] F. Petronella, S. Diomede, E. Fanizza, G. Mascolo, T. Sibillano, A. Agostiano, M.L. Curri, R. Comparelli, Photodegradation of nalidixic acid assisted by TiO2 nanorods/Ag nanoparticles based catalyst, Chemosphere, 91 (2013) 941-947.

[19] F. Vargas, C. Rivas, R. Machado, M.A. Miranda, Photodegradation of nalidixic and tiaprofenic acids and nifedipine in aerobic conditions, Photodermatol. Photoimmunol. Photomed., 8 (1991) 218-221.

[20] C. Carlesi Jara, D. Fino, V. Specchia, G. Saracco, P. Spinelli, Electrochemical removal of antibiotics from wastewaters, Appl. Catal., B, 70 (2007) 479-487.

[20] F.C. Walsh, Electrochemical technology for environmental treatment and clean energy conversion, Pure Appl. Chem., 73 (2001) 1819-1837.

[22] V.K. Gupta, R. Jain, K. Radhapyari, N. Jadon, S. Agarwal, Voltammetric techniques for the assay of pharmaceuticals—A review, Anal. Biochem., 408 (2011) 179-196.

[23] S.W. da Silva, C.R. Klauck, M.A. Siqueira, A.M. Bernardes, Degradation of the commercial surfactant nonylphenol ethoxylate by advanced oxidation processes, J. Hazard. Mater., 282 (2015) 241-248.

[24] L. Agüí, P. Yáñez-Sedeño, J.M. Pingarrón, Role of carbon nanotubes in electroanalytical chemistry: A review, Anal. Chim. Acta, 622 (2008) 11-47.

[25] Y.-P. Li, H.-B. Cao, C.-M. Liu, Y. Zhang, Electrochemical reduction of nitrobenzene at carbon nanotube electrode, J. Hazard. Mater., 148 (2007) 158-163.

[26] R.M. Cardoso, R.H.O. Montes, A.P. Lima, R.M. Dornellas, E. Nossol, E.M. Richter, R.A.A: Munoz, Multi-walled carbon nanotubes: Size-dependent electrochemistry of phenolic compounds, Eletrochim. Acta, 176 (2015) 36-43.

[27] G. Liu, S.L. Riechers, M.C. Mellen, Y. Lin, Sensitive electrochemical detection of enzymatically generated thiocholine at carbon nanotube modified glassy carbon electrode, Electrochem. Commun., 7 (2005) 1163-1169.

[28] H. Shin, J. Song, E. Shin, C. Kang, Ion-exchange adsorption of copper(II) ions on functionalized single-wall carbon nanotubes immobilized on a glassy carbon electrode, Electrochim. Acta, 56 (2011) 1082-1088.

[29] L.Q. Hoa, M.d.C. Vestergaard, H. Yoshikawa, M. Saito, E. Tamiya, Functionalized multi-walled carbon nanotubes as supporting matrix for enhanced ethanol oxidation on Pt-based catalysts, Electrochem. Commun., 13 (2011) 746-749.

[30] S.M. Ghoreishi, M. Behpour, E. Hajisadeghian, M. Golestaneh, Voltammetric determination of resorcinol on the surface of a glassy carbon electrode modified with multi-walled carbon nanotube, Arabian J. Chem., (2012) doi:10.1016/j.arabjc.2012.04.009.

[31] Y. Patiño, E. Díaz, S. Ordóñez, E. Gallegos-Suarez, A. Guerrero-Ruiz, I. Rodríguez-Ramos, Adsorption of emerging pollutants on functionalized multiwall carbon nanotubes, Chemosphere, 136 (2015) 174-180.

[32] R. García-González, A. Fernández-La Villa, A. Costa-García, M.T. Fernández-Abedul, Dispersion studies of carboxyl, amine and thiol-functionalized carbon nanotubes for improving the electrochemical behavior of screen printed electrodes, Sens. Actuators, B, 181 (2013) 353-360.

[33] B. Rezaei, S.Z. Mirahmadi Zare, Modified glassy carbon electrode with multiwall carbon nanotubes as a voltammetric sensor for determination of noscapine in biological and pharmaceutical samples, Sens. Actuators, B, 134 (2008) 292-299.

[34] L. Fotouhi, M. Alahyari, Electrochemical behavior and analytical application of ciprofloxacin using a multi-walled nanotube composite film-glassy carbon electrode, Colloids Surf., B, 81 (2010) 110-114.

[35] A.J. Bard, L.R. Faulkner, Electrochemical Methods, Wiley, New York, 2001.

[36] Y. Zeng, D. Yu, Y. Yu, T. Zhou, G. Shi, Differential pulse voltammetric determination of methyl parathion based on multiwalled carbon nanotubes–poly(acrylamide) nanocomposite film modified electrode, J. Hazard. Mater., 217–218 (2012) 315-322.

[37] R. Jain, S. Sharma, Glassy carbon electrode modified with multi-walled carbon nanotubes sensor for the quantification of antihistamine drug pheniramine in solubilized systems, J. Pharm. Anal., 2 (2012) 56-61.

[38] M. Moyo, L.R. Florence, J.O. Okonkwo, Improved electro-oxidation of triclosan at nano-zinc oxide-multiwalled carbon nanotube modified glassy carbon electrode, Sens. Actuators, B, 209 (2015) 898-905.

[39] A.G. Cabanillas, M.I.R. Cáceres, M.A.M. Cañas, J.M.O. Burguillos, T.G. Díaz, Square wave adsorptive stripping voltametric determination of the mixture of nalidixic acid and its main metabolite (7-hydroxymethylnalidixic acid) by multivariate methods and artificial neural network, Talanta, 72 (2007) 932-940.

[40] R.T. Kachoosangi, G.G. Wildgoose, R.G. Compton, Sensitive adsorptive stripping voltammetric determination of paracetamol at multiwalled carbon nanotube modified basal plane pyrolytic graphite electrode, Anal. Chim. Acta, 618 (2008) 54-60.

[41] V.K. Gupta, A.K. Jain, S.K. Shoora, Multiwall carbon nanotube modified glassy carbon electrode as voltammetric sensor for the simultaneous determination of ascorbic acid and caffeine, Electrochim. Acta, 93 (2013) 248-253.

[42] O. Lorphensri, D.A. Sabatini, T.C.G. Kibbey, K. Osathaphan, C. Saiwan, Sorption and transport of acetaminophen, 17α-ethynyl estradiol, nalidixic acid,with low organic content aquifer sand, Water Res., 41 (2007) 2180-2188.

[43] A. Afkhami, H. Ghaedi, T. Madrakian, D. Nematollahi, B. Mokhtari, Electro-oxidation and voltammetric determination of oxymetholone in the presence of mestanolone using glassy carbon electrode modified with carbon nanotubes, Talanta, 121 (2014) 1-8.

[4] B. Dogan-Topal, B. Bozal-Palabıyık, B. Uslu, S.A. Ozkan, Multi-walled carbon nanotube modified glassy carbon electrode as a voltammetric nanosensor for the sensitive determination of anti-viral drug valganciclovir in pharmaceuticals, Sens. Actuators B: Chemical, 177 (2013) 841-847.

[45] W.-S. Zhou, B. Zhao, X.-H. Huang, X.-D. Yang, Electrochemical Determination of 4-Nonylphenol on Graphene-Chitosan Modified Glassy Carbon Electrode, Chin. J. Anal. Chem., 41 (2013) 675-680.

[46] M. Rizk, H.A.M. Hendawy, M.M. Abou El-Alamin, M.I. Moawad, Sensitive anodic voltammetric determination of methylergometrine maleate in bulk and pharmaceutical dosage forms using differential pulse voltammetry, J. Electroanal. Chem., 749 (2015) 53-61.

[47] Q. Zheng, P. Yang, H. Xu, J. Liu, L. Jin, A simple and sensitive method for the determination of 4-n-octylphenol based on multi-walled carbon nanotubes modified glassy carbon electrode, J. Environ. Sci., 24 (2012) 1717-1722.

[48] J.A. Rather, K. De Wael, C60-functionalized MWCNT based sensor for sensitive detection of endocrine disruptor vinclozolin in solubilized system and wastewater, Sens. Actuators B: Chemical, 171–172 (2012) 907-915.

[49] R. Jain, J.A. Rather, Voltammetric determination of antibacterial drug gemifloxacin in solubilized systems at multi-walled carbon nanotubes modified glassy carbon electrode, Colloids Surf. B: Biointerfaces, 83 (2011) 340-346.

[50] R.H. Patil, R.N. Hegde, S.T. Nandibewoor, Electro-oxidation and determination of antihistamine drug, cetirizine dihydrochloride at glassy carbon electrode modified with multi-walled carbon nanotubes, Colloids Surf. B: Biointerfaces, 83 (2011) 133-138.

[51] A.C. Pereira, A.d.S. Santos, L.T. Kubota, Electrochemical behavior of riboflavin immobilized on different matrices, J. Colloid Interface Sci., 265 (2003) 351-358.

[52] H.-H. Cho, B.A. Smith, J.D. Wnuk, D.H. Fairbrother, W.P. Ball, Influence of Surface Oxides on the Adsorption of Naphthalene onto Multiwalled Carbon Nanotubes, Environ. Sci. Technol., 42 (2008) 2899-2905.

[53] J. Wang, Z. Chen, B. Chen, Adsorption of Polycyclic Aromatic Hydrocarbons by Graphene and Graphene Oxide Nanosheets, Environ. Sci. Technol., 48 (2014) 4817-4825.

[54] W. Yan, L. Yan, J. Duan, C. Jing, Sorption of organophosphate esters by carbon nanotubes, J. Hazard. Mat., 273 (2014) 53-60.

[55] H. Bi, Y. Li, S. Liu, P. Guo, Z. Wei, C. Lv, J. Zhang, X.S. Zhao, Carbon-nanotube-modified glassy carbon electrode for simultaneous determination of dopamine, ascorbic acid and uric acid: The effect of functional groups, Sens. Actuators B: Chemical, 171–172 (2012) 1132-1140.

[56] B. Habibi, M.H. Pournaghi-Azar, Simultaneous determination of ascorbic acid, dopamine and uric acid by use of a MWCNT modified carbon-ceramic electrode and differential pulse voltammetry, Electrochim. Acta, 55 (2010) 5492-5498.

[57] G. Laera, D. Cassanot, A. Lopez, A. Pinto, A. Pollice, G. Ricco, G. Mascolo, Removal of organics and degradation products from industrial wastewater by a membrane bioreactor integrated with ozone or UV/H2O2 treatment, Environ. Sci. Technol. 42 (2012) 1010-1018.

Table 1. Multi-wall carbon nanotubes film properties

Material	Density (g·cm^{-3})	Film tickness (μm)	Surface area (cm^2)
Bare	-	-	0.064
MWCNT	0.198	0.90	0.180
MWCNT-COOH	0.140	0.58	0.070
MWCNT-NH_2	(0.09[1]-0.23[2])	(0.77[1]-1.84[2])	0.069

[1] Perimeter zone
[2] Central zone

Figure captions

Figure 1. SEM images of working electrodes (A) Bare-GCE, (B) MWCNT modified GCE, (C) MWCNT-COOH modified GCE and (D) MWCNT- NH_2 modified GCE.

Figure 2. SEM images fil thickness for: (A) MWCNT modified GCE, (B) MWCNT-COOH modified GCE and (C) MWCNT- NH_2 modified GCE.

Figure 3. Cyclic voltammogram of bare GCE in blank solution (·····) and in the presence of $1E^{-5}$ M of NAL (—), both in PBS buffer (pH=7.0) and scan rate: 50 mVs^{-1}.

Figure 4. Electrocatalytic effect of GCE-MWCNTs on $1E^{-5}$ M NAL by DPV on (·····) bare GCE and (—) modified GCE with MWCNTs in PBS buffer (pH=7.0) and scan rate: 50 mVs^{-1}.

Figure 5. Plot between peak current versus concentration as obtained in reduction of NAL by DPV in the optimal conditions using MWCNT-GCE.

Figure 6. Effect of pH on peak current of 1×10^{-5} M NAL in PBS at the MWCNT-GCE electrode and scan rate of 50 mVs^{-1}. pH=3 **– · – ·** , pH=5 **—**, pH=7 **- - -**, pH=9 **···**.

Figure 7. Effect of the deposition time on the peak height on DPV of 1×10^{-5}M NAL in PBS (pH=5.0) and 50 mVs^{-1} of scan rate

Figure 8. Electrocatalytic effect of GCE modified with functionalized-MWCNT of 1×10^{-5} M NAL in PBS (pH=5.0). Bare **– · – ·** , MWCNT **—**, MWCNT-COOH **- - -**, MWCNT-NH_2 **···**

Figure 8. Peak current versus concentration as obtained in reduction of NAL by DPV in the optimal conditions.

Figure 9. Electrochemical degradation of 1×10^{-5}M NAL, (A) constant V/A ratio and different DPV cycles and (B) 15 DPV and different V/A ratio, both at the optimum experimental conditions.

Figure 10. Proposed NAL degradation pathway 1 by DPV

Figure 11. Proposed NAL degradation pathway 2 by DPV

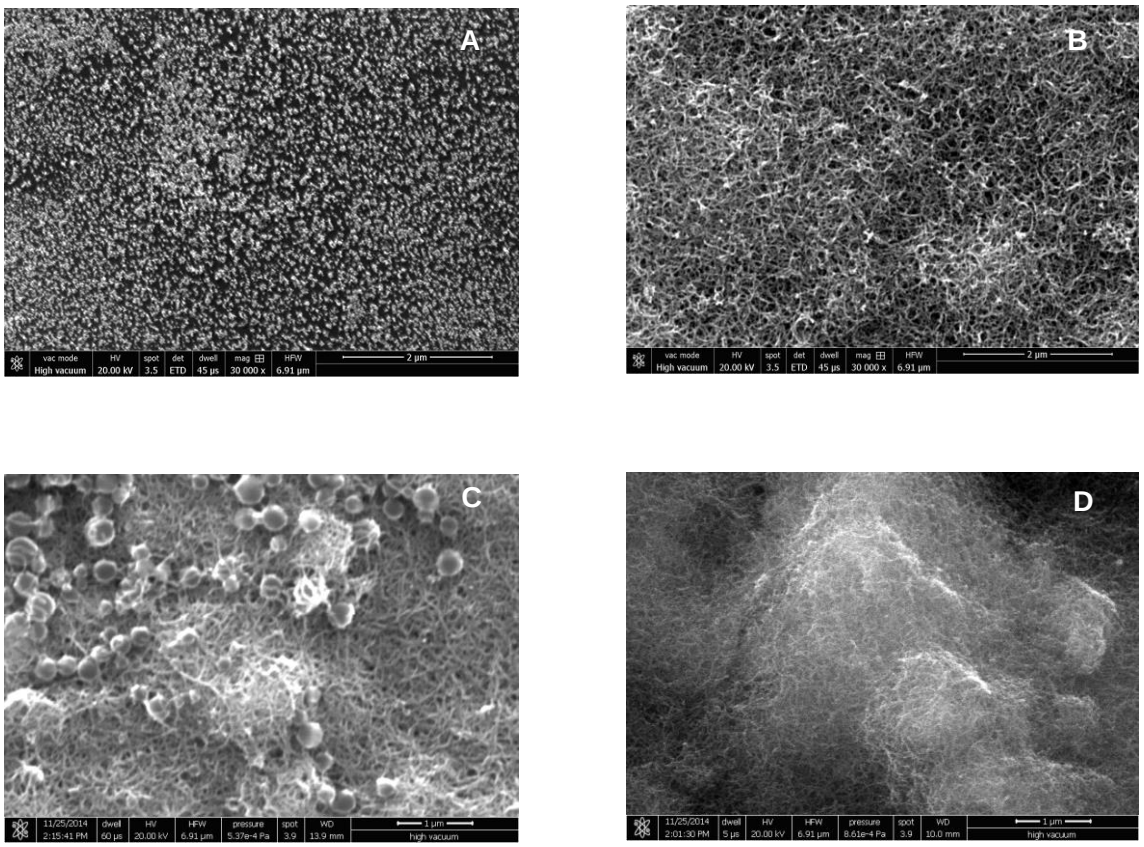

Figure 1. SEM images of working electrodes: (A) Bare-GCE, (B) MWCNT modified GCE, (C) MWCNT-COOH modified GCE and (D) MWCNT- NH_2 modified GCE.

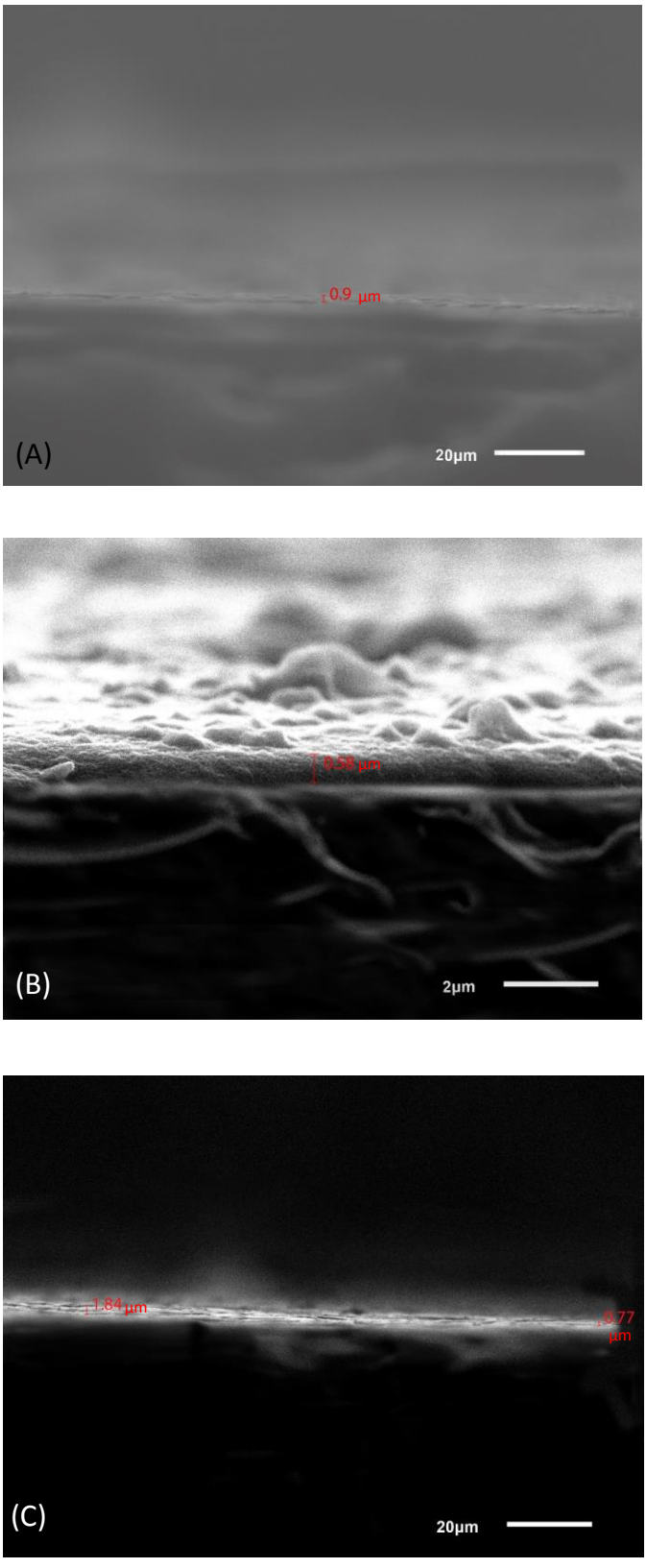

Figure 2. SEM images film thickness for: (A) MWCNT modified GCE, (B) MWCNT-COOH modified GCE and (C) MWCNT- NH_2 modified GCE.

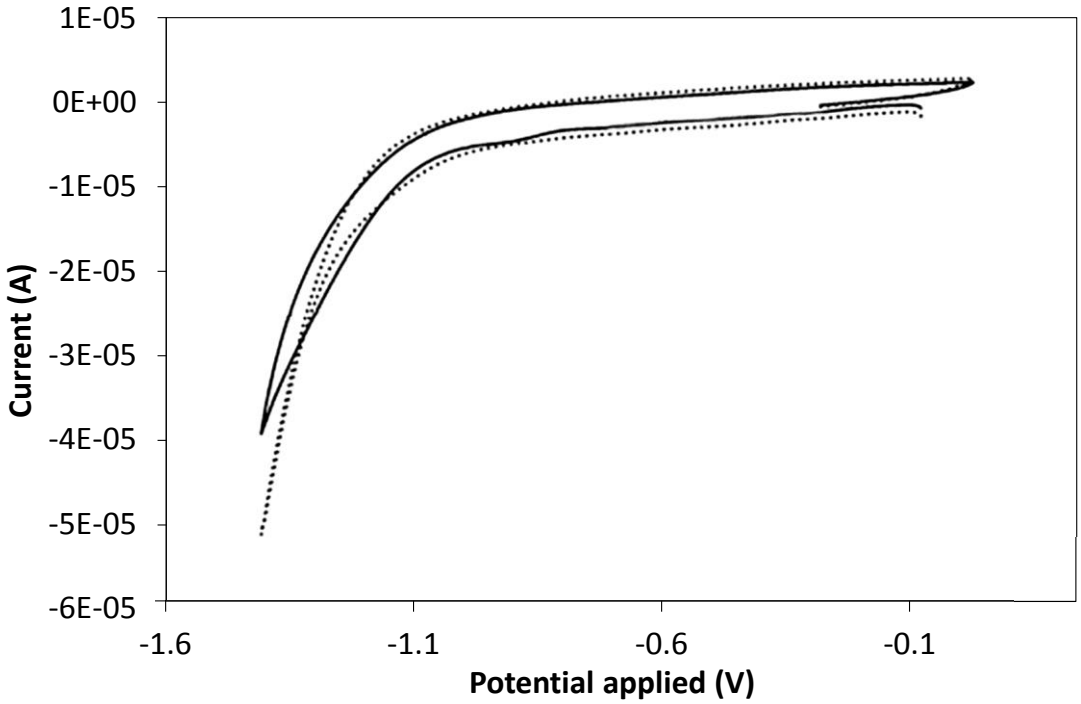

Figure 3. Cyclic voltammogram of bare GCE in blank solution (dotted line) and in the presence of $1E^{-5}$ M of NAL (solid line), both in PBS buffer (pH=7.0) and scan rate: 50 mVs^{-1}

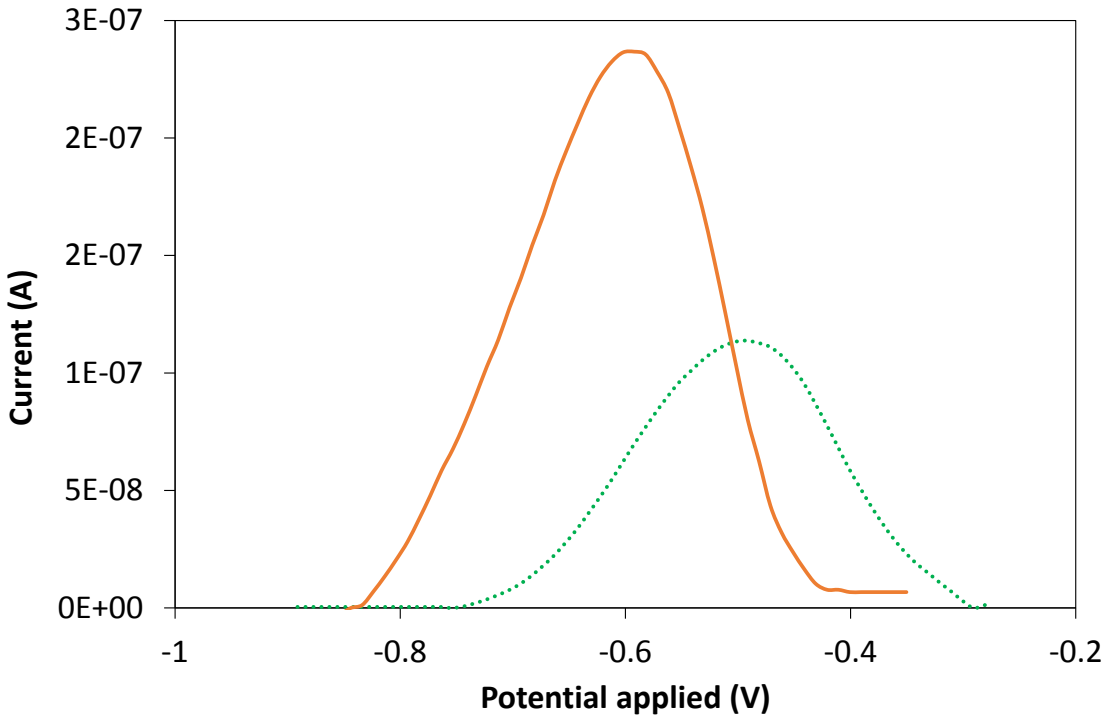

Figure 4. Electrocatalytic effect of GCE-MWCNTs on $1E^{-5}$ M NAL by DPV on (dotted line) bare GCE and (solid line) modified GCE with MWCNTs in PBS buffer (pH=7.0) and scan rate: 50 mVs^{-1}.

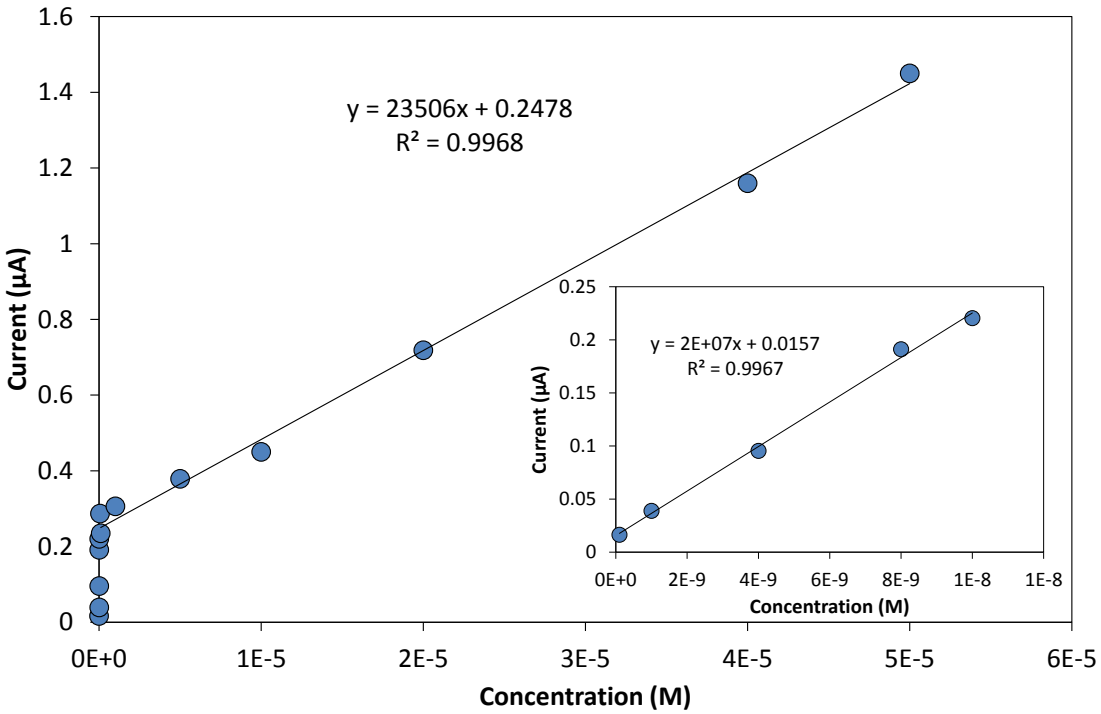

Figure 5. Plot between peak current versus concentration as obtained in reduction of NAL by DPV in the optimal conditions using MWCNT-GCE.

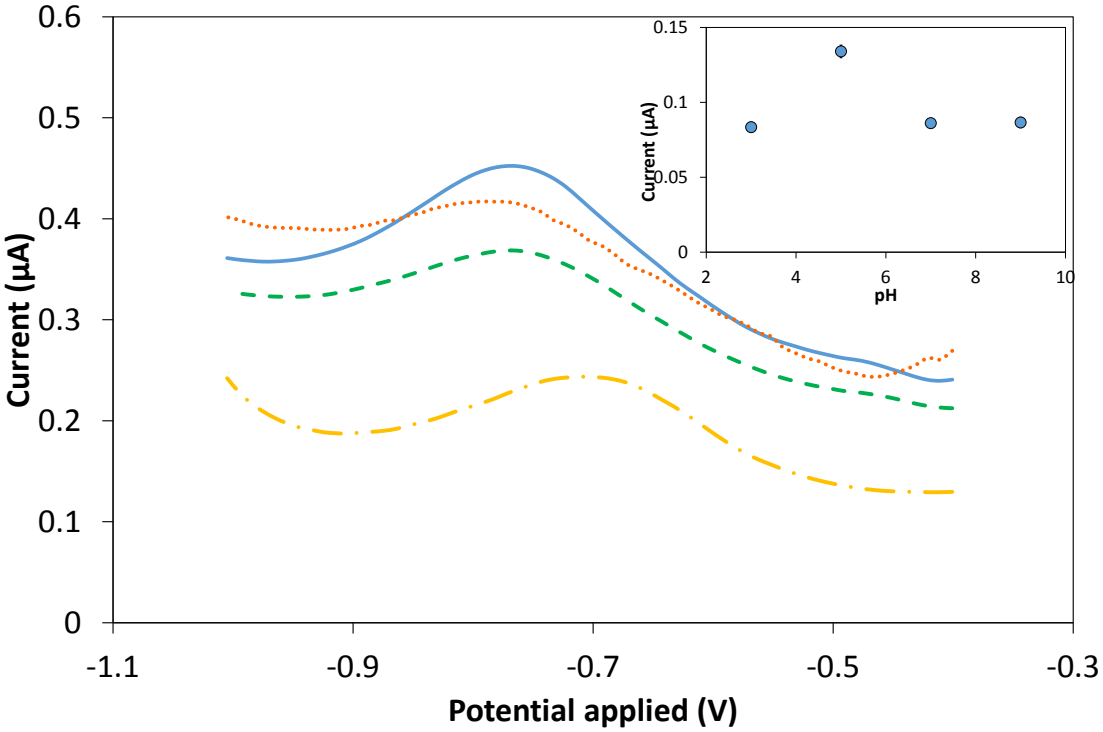

Figure 6. Effect of pH on peak current of 1×10^{-5} M NAL in PBS at the MWCNT-GCE electrode and scan rate of 50 mVs^{-1}. pH=3 – · – · , pH=5 —, pH=7 - - -, pH=9 ⋯.

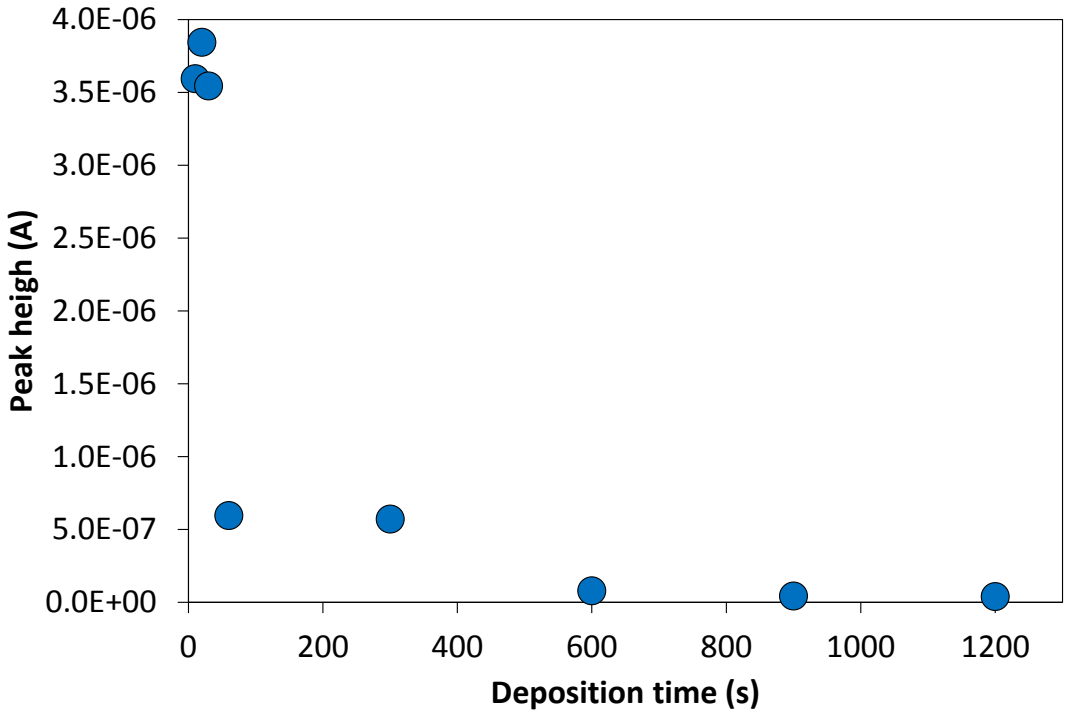

Figure 7. Effect of the deposition time on the peak height on DPV of 1×10^{-5}M NAL in PBS (pH=5.0) and 50 mVs^{-1} of scan rate

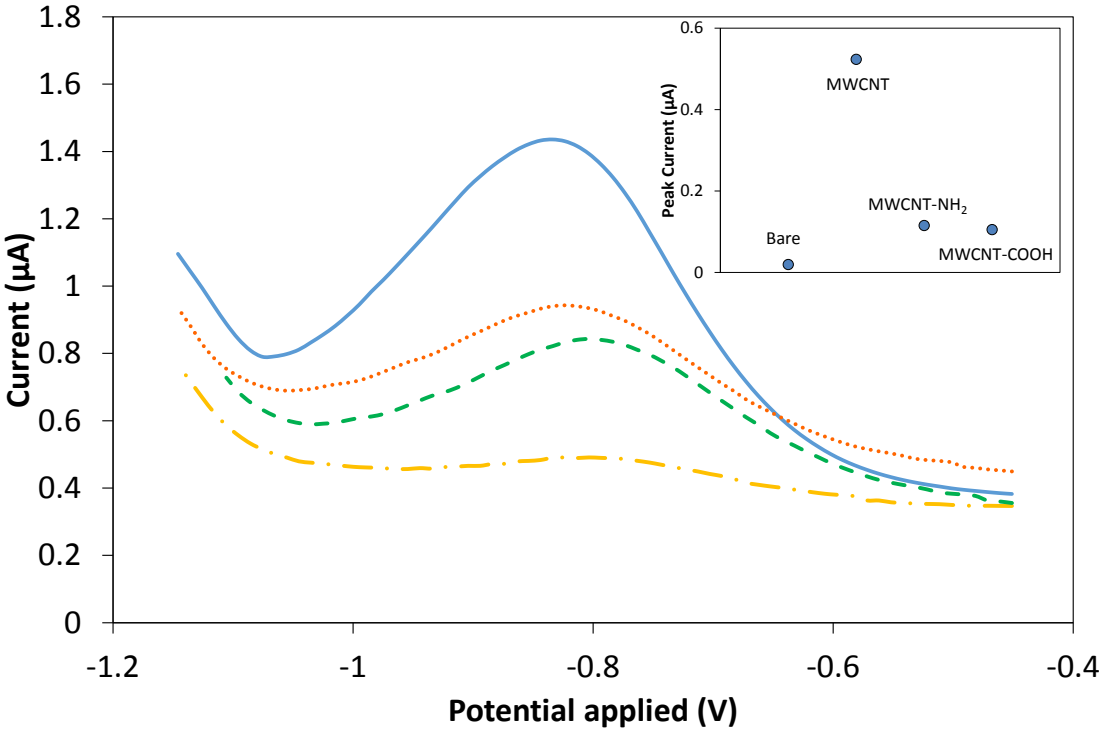

Figure 8. Electrocatalytic effect of GCE modified with functionalized-MWCNT of 1×10^{-5} M NAL in PBS (pH=5.0). Bare – · – · , MWCNT —, MWCNT-COOH - - -, MWCNT-NH_2 ··· .

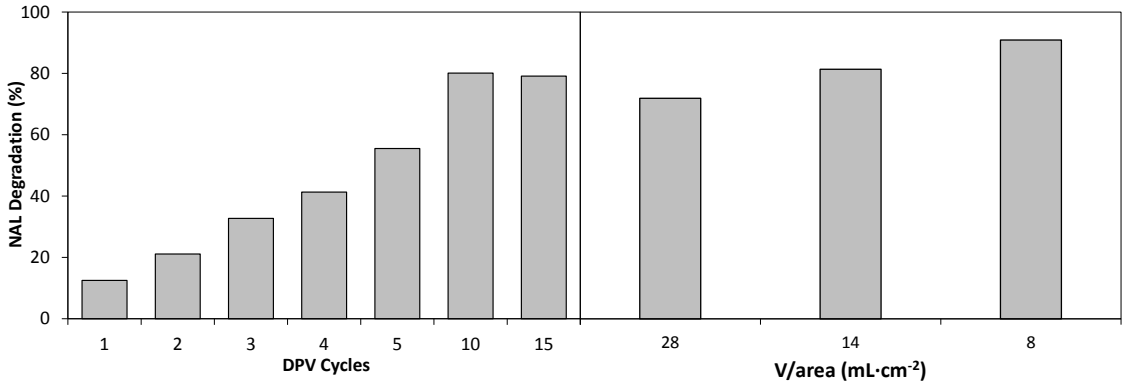

Figure 9. Electrochemical degradation of 1×10^{-5}M NAL, (A) constant V/A ratio and different DPV cycles and (B) 15 DPV and different V/A ratio, both at the optimum experimental conditions

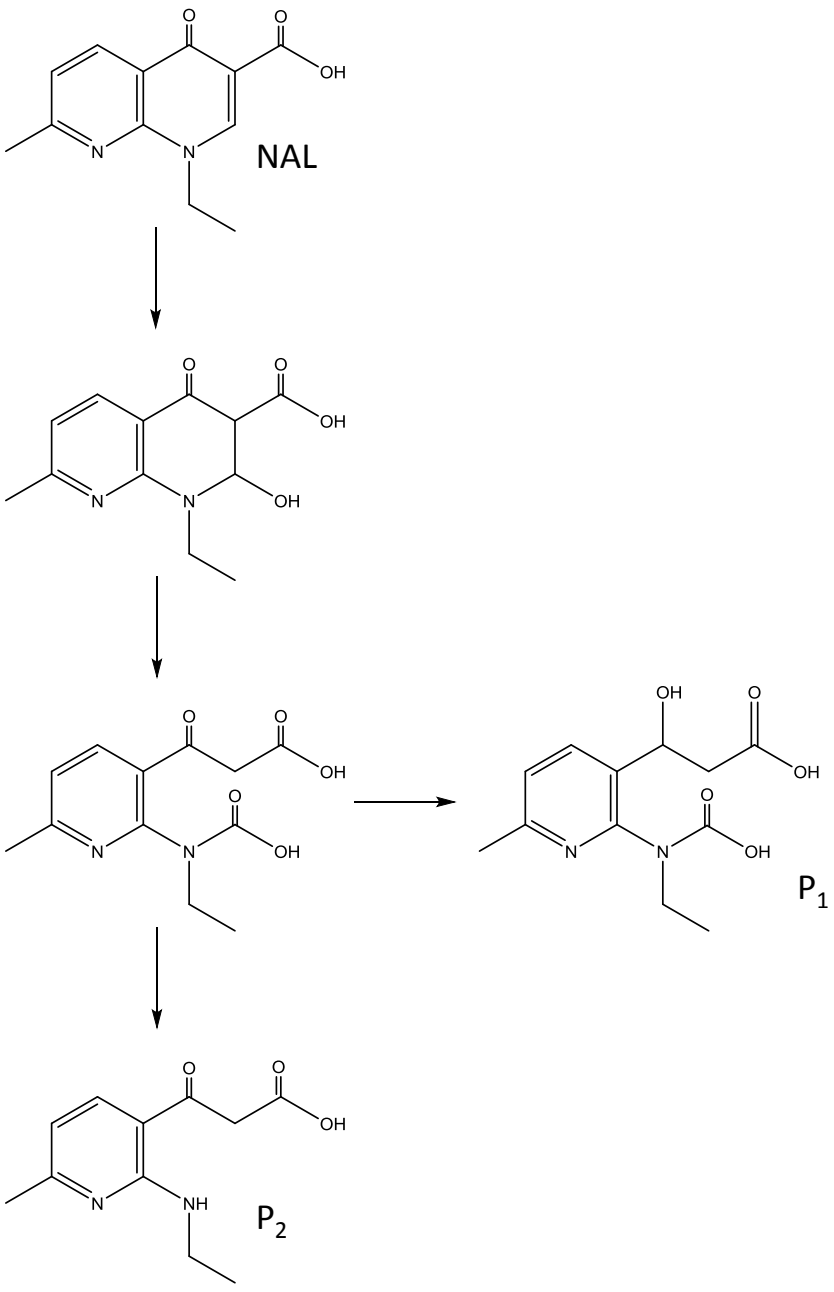

Figure 10. Proposed NAL degradation pathway 1 by DPV

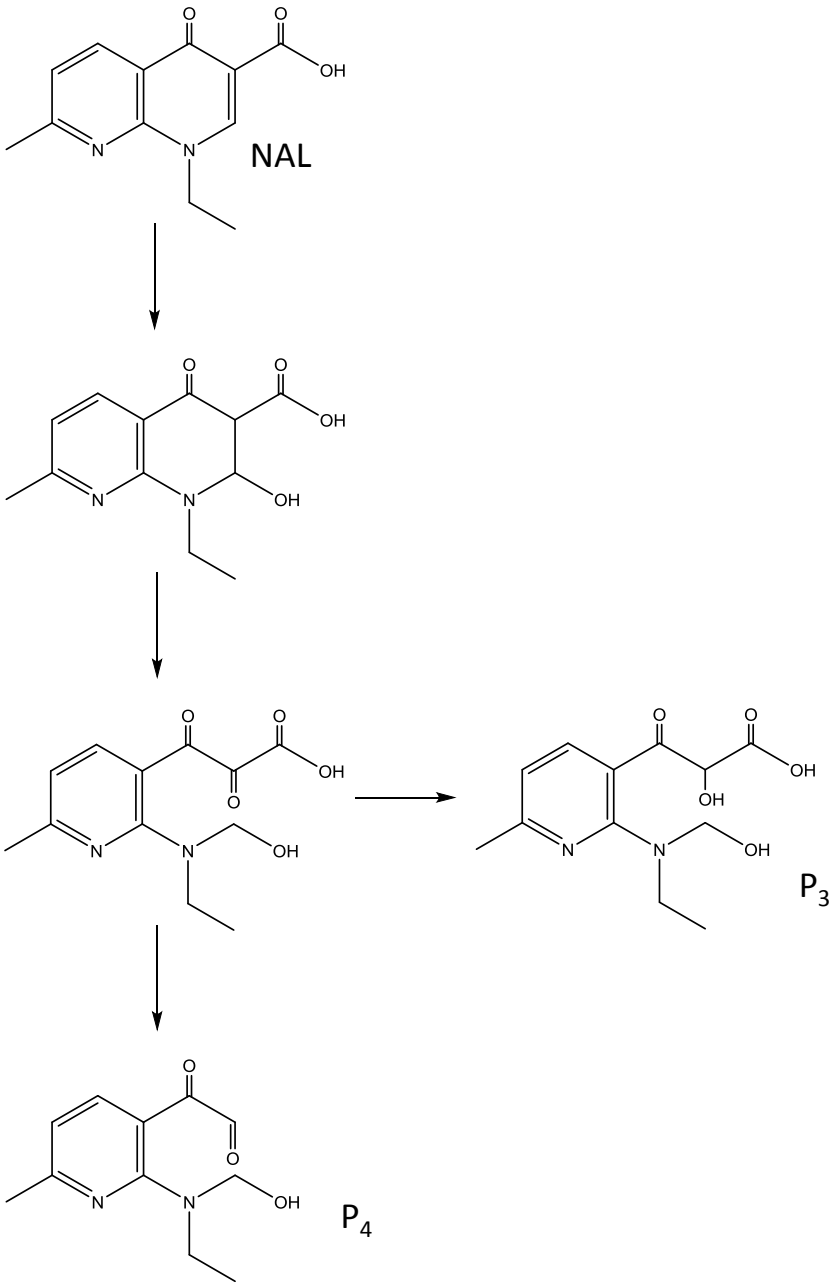

Figure 11. Proposed NAL degradation pathway 2 by DPV